Nanoscale Res Lett (2010) 5:839–845
DOI 10.1007/s11671-010-9572-7

NANO EXPRESS

Effects of the Template Composition and Coating on the Photoluminescence Properties of ZnS:Mn Nanoparticles

Lingling Peng · Yuhua Wang

Received: 16 December 2009 / Accepted: 26 February 2010 / Published online: 16 March 2010

Abstract Mn-doped ZnS nanocrystals based on low dopant concentrations (0–2%) and coated with a shell of $Zn(OH)_2$ have been prepared via soft template and precipitation reaction. The results indicate that the ZnS:Mn nanocrystal is cubic zinc blende structure and its diameter is 3.02 nm as demonstrated by XRD. Measured by TEM, the morphology of nanocrystals is a spherical shape, and their particle size (3–5 nm) is similar to that of XRD results. Photoluminescence spectra under ultraviolet region shows that the volume ratio of alcohol to water in the template has a great effect on the luminescence properties of ZnS:Mn particles. Compared with unpassivated ZnS:Mn nanocrystals, ZnS:Mn/$Zn(OH)_2$ core/shell nanocrystal exhibits much improved luminescence and higher absolute quantum efficiency. Meanwhile, we simply explore the formation mechanism of ZnS:Mn nanocrystals in alcohol and water system and analyze the reason why alcohol and water cluster structures can affect the luminescent properties of nanoparticle.

Keywords ZnS · Nanoparticals · Coating · Template · Photoluminescence

Introduction

The preparation and characterization of II–VI nanoscale semiconductor compounds have attracted much attention over the past few years due to their fundamental properties [1] and applications, mostly as tunable emitters for biomedical labeling [2], light emitting diodes (LED), lasers, and sensors [3–5]. The intrinsic toxicity of cadmium has cast a doubtful future in this promising field. However, wide band gap semiconductor nanocrystals, such as zinc chalcogenide ones doped with transition metal ions [6, 7, 9–11], may overcome this concern and yet maintain the advantages of the nanocrystal emitters. In 1994, Bhargava et al. [8] initiatively proposed luminescence properties of Mn-doped ZnS nanocrystals that were prepared by a room temperature chemical process. Then, nanocrystalline ZnS has been widely and deeply investigated [12] since nanosized ZnS can be easily prepared. As a typical II–VI semiconductor, ZnS, especially doped with divalent manganese ions, has been commercially used as a phosphor as well as in thin film electroluminescent devices. In the bulk form, ZnS is an interesting II–VI semiconductor with a large band gap 3.68 eV (340 nm). At the nanometer scale, ZnS has attracted more attention due to its interesting optical, electric properties, and large quantum efficiencies depending on its size. For instance, it can be used as a higher band gap material to passivate other quantum semiconductor heterostructure to increase their quantum yields [13]. The properties of the photoluminescent and electroluminescent materials could be greatly affected by doping concentration of Mn. The Mn ion, used as a dopant in many luminescent materials, has a d^5 configuration that exhibits a broad emission peak, and its position strongly depends on the host lattice, which lies on the change in strength of crystal field with host. The emission color can vary from green to deep red, corresponding to a $^4T_1$–$^6A_1$ transition. To obtain nanometer-sized particles, a variety of methods have been proposed, including microemulsion method [14], sol–gel processing [15], competitive reaction chemistry method [16], and aqueous chemical method [17].

L. Peng · Y. Wang (✉)
Department of Materials Science, School of Physical Science and Technology, Lanzhou University, 730000 Lanzhou, People's Republic of China
e-mail: wyh@lzu.edu.cn

Since Dixit et al. [18] observed molecular segregation in a concentrated alcohol–water(A/W) solution, there have been few reports on generating of nano-crystallined CeO_2 and silicon in A/W mixed solvents [19] or in ethylalcohol liquid bridges [20]. In this paper, we focus on preparation of stabilized Mn-doped ZnS nanocrystals by soft template method and coated $Zn(OH)_2$ shells through precipitation reaction. Photoenhanced luminescence and higher quantum efficiency have been observed in ZnS:Mn/$Zn(OH)_2$ nanoparticle.

Experimental Procedure

$Zn(CH_3COO)_2{\cdot}2H_2O$(A.R.), $Na_2S{\cdot}9H_2O$(A.R.), and $Mn(CH_3COO)_2{\cdot}4H_2O$(A.R.) were employed as raw materials and C_2H_5OH and H_2O mixed solution as soft template. First, Na_2S and dopant precursor $Mn(CH_3COO)_2$ were ground in mortar to form MnS crystal nucleus, and C_2H_5OH and H_2O solutions were added as soft template in grinding process. Then, $Zn(CH_3COO)_2$ was added and ground in soft template for the regrowth of ZnS on the surface of MnS layer. The concentration of the dopant in the nuclei can be regulated varying the precursor ratio. The products were collected by centrifugal sedimentation and first washed by ionized water then by alcohol. Finally, the products were ultrasonically dispersed in alcohol and dried at 40°C in vacuum.

$Zn(OH)_2$ shell, coating on ZnS:Mn nanocrystals can be produced as follows: ZnS:Mn nanocrystal was put into deionized water and ultrasonically dispersed for 2 h. Appropriate amount of $Zn(CH_3COO)_2$ aqueous solution was slowly dropped into the ZnS:Mn suspension under the conditions of vigorous stirring. Ten minutes later, appropriate amount of NaOH aqueous solution was dropped into the suspension to form stoichiometric $Zn(OH)_2$. After 1 h of continuous stirring, the resulting precipitates were dealt in the same way as the ZnS:Mn nanocrystals.

All the samples were characterized by powder X-ray diffraction (XRD) using a Rigaku diffractometer with Ni-filtered CuKa radiation at room temperature. The transmission electron microscopy (TEM) images of the nanoparticles were obtained by using TEM (JEM-2100F Electron Microscope/JEOL Co. 200 kV). The optical properties of finely ground samples were collected by an UV–vis spectrophotometer (PE lambda950) using BaSO4 as a reference in the range of 200–700 nm. The photoluminescence (PL) spectra in the UV region were obtained using a FLS-920T fluorescence spectrophotometer equipped with Xe 900 (450 W xenon arc lamp) as the light source with spectral slits width of 1 nm. The quantum yield of the samples excited at 300 nm was recorded with HORIBA JOBIN-YVON Fluorlog-3 spectrofluorometer system. All the spectra were recorded at room temperature.

Result and Discussion

The Volume Ratio of A/W is 1:1

The XRD patterns of the ZnS:Mn nanocrystals prepared in the condition of alcohol and water volume ratio of 1:1 are presented in Fig. 1. The broadening of the diffraction peaks of all the Mn:ZnS nanoparticles, a characteristic of nanocrystal, can be obviously observed. For all the samples, the main three diffraction peak positions correspond to the lattice planes of (111), (220), and (311), matching the cubic zinc blende ZnS structure (JCPDS No. 05-0566). No diffraction peaks from manganese impurities were detected. It indicates that the Mn ions are dispersed into the ZnS matrix. According to the Debye–Scherrer formula $d = k\lambda/\beta\cos\theta$,, the mean crystalline sizes calculated from the full-width at half-maximum (FWHM) of these lines were about 3.02 nm.

This paper extends the method employing the A/W template to produce the ZnS:Mn nanocrystals. Figure 2 shows the TEM image of sample for 2% Mn concentration. The nanocrystals distribute in a narrow size; the shape of the particles is approximately spherical, and the mean diameter is about 3–5 nm. The nucleus formation mechanism in alcohol and water system is as follows: the reagents are over saturation in A/W template, and the relationship between super saturation and the radius of stable nuclei (r) can be expressed by Kelvin equation:

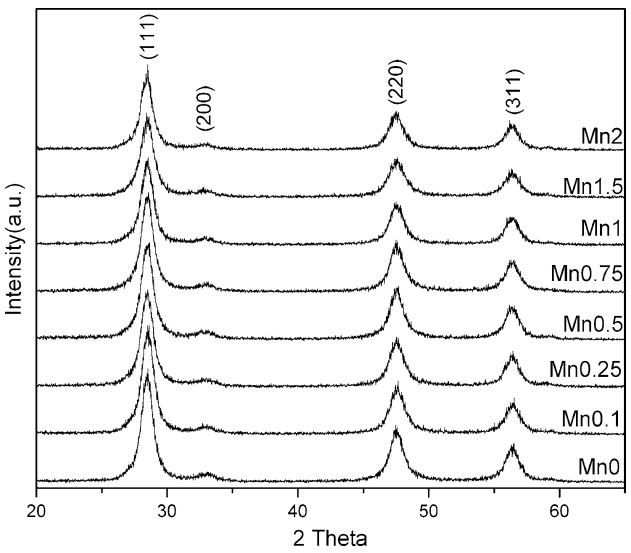

Fig. 1 XRD patterns of ZnS:Mn nanocrystals (A/W = 1:1)

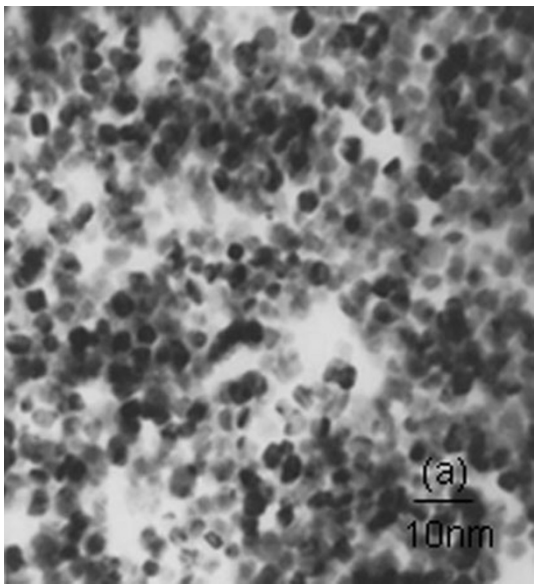

Fig. 2 TEM image of ZnS:Mn nanocrystals (A/W = 1:1)

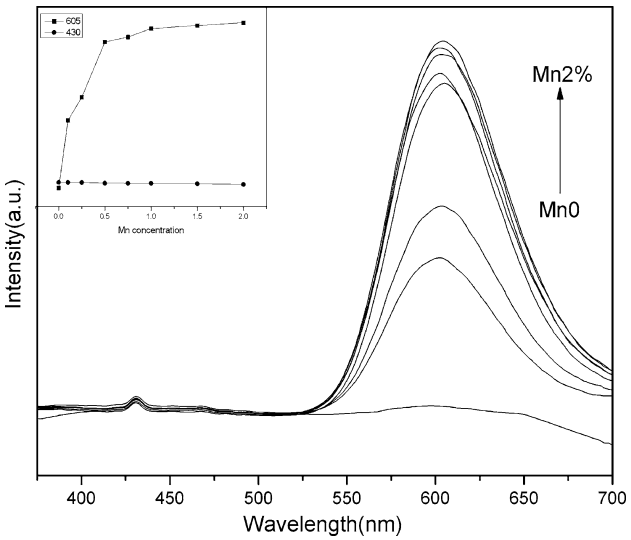

Fig. 3 The emission spectra of ZnS:Mn nanocrystals for different Mn concentrations (inset is the intensity of emission as a function of Mn concentration)

$$r = \frac{2m\gamma}{kT\rho \ln S} \tag{1}$$

The degree of super saturation (S) is defined by the ratio of solute concentration (C) and saturation concentration (C_1):

$$S = \frac{C}{C_1} \tag{2}$$

when the S value is much larger than unity, a great number of primary nuclei formed. According to [20], the dependence of particle radius (r) on the dielectric constant (ε) of the solution can be further simplified as

$$\frac{1}{r} = A + \frac{B}{\varepsilon}, \tag{3}$$

$$A = \frac{kT\rho}{2m\gamma \ln C},\ B = \frac{\rho z_+ z_- e^2}{8\pi m\gamma \varepsilon_0 (r_+ + r_-)} \tag{4}$$

where ε_0 is the permittivity in vacuum and ε is the dielectric constant in a given solution. The symbols r_+ and r_- represent the radii of ions charged z_+ and z_-, respectively, and e represents the elementary charge ($e = 1.602 \times 10^{-19}$ C).

For mixed solvents of homologous alcohol and water system, values of A and B can be regarded as constants. Therefore, it is clear that the change in the dielectric constant of mixed solvent can remarkably affect the nucleation rate and the particle size. In addition, for single water system, due to the small particle size there is a big specific surface area, so the products easily aggregate. Because alcohol and water can dissolve each other unlimitedly, most of water molecules adsorbing on the particle surface can be replaced by alcohol molecules, which diminish the particle surface tension and surface energy; thus, the trend of reunion between the particles can be effectively declined. Besides, the probability of collisions between particles can be reduced by the steric effect of organic system (A/W), which contributes to the formation of nanoparticles with uniformity and good dispersion.

Figure 3 illustrates photoluminescence (PL) spectra of ZnS:Mn nanocrystals with different Mn concentration excited at 300 nm in the room temperature. The PL spectrum shows a weak emission at 430 nm and a broad strong emission band ranging from 520 to 700 nm. The weak blue-light emission at 430 nm is attributed to a defect related emission of the ZnS host [11]. The orange broad emission centering at 605 nm ascribes to the transition of Mn from the first excited state of $^4T_1$ to the ground state of $^6A_1$. The origin of typical emission of Mn is as follows: when Mn ions are incorporated into the ZnS lattice and substitute for host cation sites; the hybrid between the sp electrons of the host ZnS and the d electrons of Mn occurs and makes the forbidden transition of $^4T_1$–$^6A_1$ partially allowed, as a result of the characteristic emission of Mn [21]. It is observed that the strong PL position from ZnS:Mn nanocrystals compared with other results [21] redshifts to 605 nm (Fig. 3). A possible explanation is that the enhancement of quantum effect in nanocrystals increases the hybrid effect, according to Tanabe-Sugano cryatal field theory of transition metal, $^4T_1$ energy in first excited state of Mn decreases with the increase in crystal field intensity, but ground state $^6A_1$ is not changed, so the shrunken gap between $^4T_1$ and $^6A_1$ causes a PL red shift.

The doped manganese in the precursors may be introduced into inside or outside of ZnS nanocrystals. Sooklal et al. [22] studied the effect of the location of Mn on the photophysics of ZnS nanocrystals. They found that whether

Mn incorporates into the ZnS lattice will lead to the orange emission, while ZnS with Mn on the surface-bound will yield the ultraviolet emission. Narayan Pradhan studied the possible nucleation and growth process, they found that the successful doping and decoupling of doping must fulfill following conditions: with the increase in doped ions, the steady increase in the PL intensity from the doping centers at about 605 nm, the fixed PL positions of the host ZnS nanocrystals and the doping centers, and the gradual decrease in the PL intensity of the host ZnS nanocrystals [23]. Inset of Fig. 3 demonstrates the functional relation between characteristic emission intensity of Mn and doping amount. According to inset of Fig. 3, with the increase in Mn, the emission intensity also increases and reaches its highest intensity at the Mn content of 2%. At the same time, emission intensity of the host ZnS nanocrystals decreased. Compared with Zn, Mn is a harder Lewis acid. Therefore, the Mn precursor would be much less than Zn if they both have the same carboxylate ligand [23]. From above all, it can be concluded that the Mn ions in our samples are indeed introduced into the host ZnS nanocrystals. From the Fig. 3, the highest doping amount is 2%.

Effect of Volume Ratio of A/W on Luminescence Behavior

At the same time, the amount of alcohol will affect the degree of agglomeration of nanoparticles. According to DLVO theory, the energy barrier between two particles that inhibits agglomeration can be expressed as [24]:

$$V = -\frac{A\kappa r}{12} + 2\pi\varepsilon_0\varepsilon_r r\Psi^2 \quad (5)$$

where A is the effective Hamaker constant, k is the Debye–Huckel parameter, r is the particle diameter, ε_r is the relative dielectric constant of the liquid medium, ε_0 is the dielectric constant of vacuum, and Ψ is the surface potential. The dielectric constant of an A/W mixed solvent decreases with an increase in the volume ratio of A/W. In this study, we kept the total A/W volume as a constant then adjusted the alcohol ratio in the template and investigated the effects of the alcohol volume on the PL properties. Mn concentration is fixed at 2%, the PL spectra of nanocrystals with various s are shown in Fig. 4. The emission intensity of ZnS:Mn enhances gradually with the increase in alcohol concentration. Because of the integrity of a better particle namely passivated surface defect, the strongest emission could be obtained when the concentration of alcohol reached 33% (alcohol and water volume ratio of 1:2, inset of Fig. 4). Then the intensity degreases gradually.

According to the results, we draw a conclusion from the process of preparing nanocrystals that the function of A/W mixed system is as follows: at that moment, the hydrogen

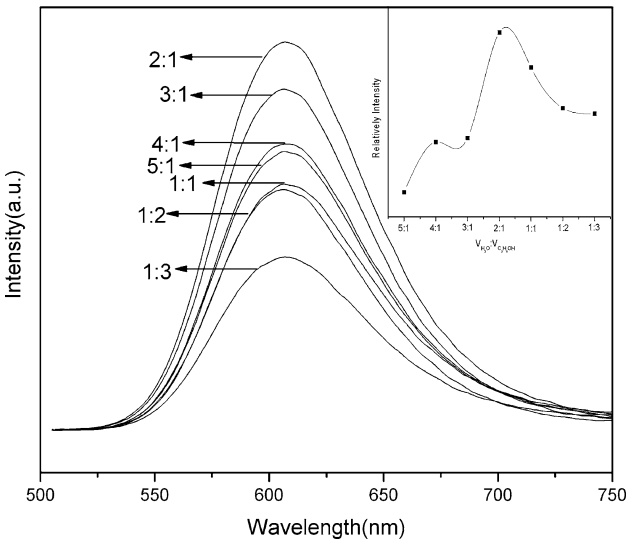

Fig. 4 The emission spectra of ZnS:Mn nanocrystals for different A/W volume ratio (inset is the intensity of emission as a function of alcohol content in template)

bonds, hydration, and ethanol–water molecules are no longer separate water molecules or ethanol molecules but bridged molecular clusters formed by a number of ethanol molecules and water molecules. It is deduced that there are three possible cluster structures [25]: five ethanol molecules and six water molecules connect with each other to form a ring or chain structure through the hydrogen bond; an ethanol molecule and two water molecules form the chain structure with hydrogen bond; and an ethanol molecule and five water molecules link mutually to form a new molecular structure. When the solution has a 60% (vol) of ethanol, the concentration of the first component cluster arrives at the maximum, the second and third types of the component cluster are, respectively, correspond to the alcohol concentration of 40 and 80%. From experiment results, it could be inferred that in the course of obtaining integrated particle crystallization, the second cluster structure is the best template, because our sample with best emission intensity was produced in the condition of the closest approach to the second type molecular structure of alcohol (40%).The optimal volume of A/W is 1:2.

Optical absorption spectra of ZnS:Mn nanocrystals for different A/W are shown in Fig. 5. It displays an excitonic absorption peak at about 300. The excitonic absorption peaks for all these samples are blueshifted in the comparison with the bulk band gap (3.68 eV corresponding to the absorption edge at 336 nm [26]). It is clearly indicated the strong quantum size effects, and they have nearly the same particle size. According to the effective mass model, the radius of the particle is related to the absorption band. The bandgap energy of nanocrystals as a function of their size is given by the Brus equation [27],

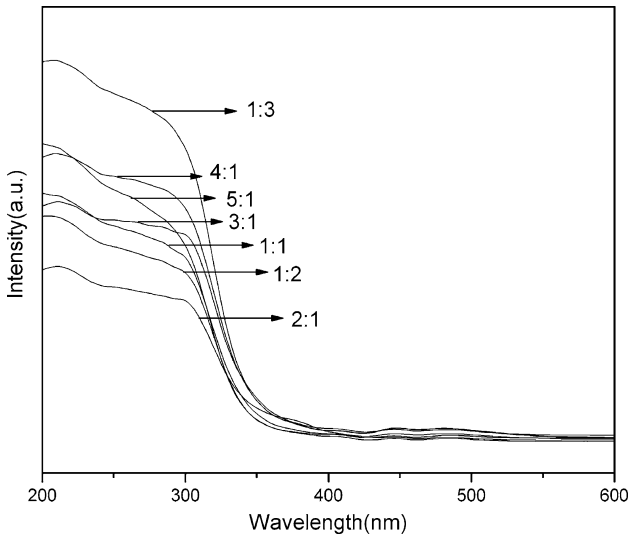

Fig. 5 The absorption spectra of ZnS:Mn nanocrystals for different A/W volume ratio

$$E = E_e + E_g = Eg + \frac{h^2\pi^2}{2R^2}\left(\frac{1}{m_e} + \frac{1}{m_h}\right) - \frac{1.8e^2}{\varepsilon R} \quad (6)$$

In the case of ZnS, using a gap Eg (bulk) = 3.68 eV, an effective mass for electrons m_e and holes $m_h = 0.61m_0$ (m_0 is the electron mass) and a dielectric constant $\varepsilon_r = 8.9$, the following relation between the bandgap Eg (R), in electron volt, and the particle radius R, in nanometers, is obtained:

$$Eg(R) \approx 3.68 - 0.3/R + 1.5/R^2 \quad (7)$$

R was calculated ranges from 1.5 to 2.5 nm (a diameter from 3 to 5 nm), in reasonable agreement with the XRD results.

Due to the sample synthesized in A/W volume ratio of 1:2 has the highest emission intensity and lowest absorption intensity (Figs. 4, 5), we can draw a conclusion that in our samples, this one has the best quantum efficiency, then we made surface treatment on this sample to improve its emission intensity and measure the quantum efficiency. That is coated with a layer of $Zn(OH)_2$ on the surface of ZnS:Mn. Figure 6 is the TEM image of ZnS:Mn coated with $Zn(OH)_2$ in A/W volume ratio of 1:2 and electron diffraction in the inset (right), while inset (left) is the image of bare ZnS:Mn nanoparticle. The results indicate that ZnS:Mn/$Zn(OH)_2$ nanoparticles with high distribution, and no aggregation was synthesized successfully. TEM shows the presence of $Zn(OH)_2$ coating layer on the surface of the ZnS:Mn. Figure 7 shows the emission spectra of two samples before and after coating. It is found that the emission intensity of coated sample enhanced by 30%. It is proven that the ZnS:Mn surface had been modified by $Zn(OH)_2$ layer. Figure 8 is the results of quantum efficiency. (a) is the scatter spectra and (b) is the emission spectra of samples. The quantum efficiency can be

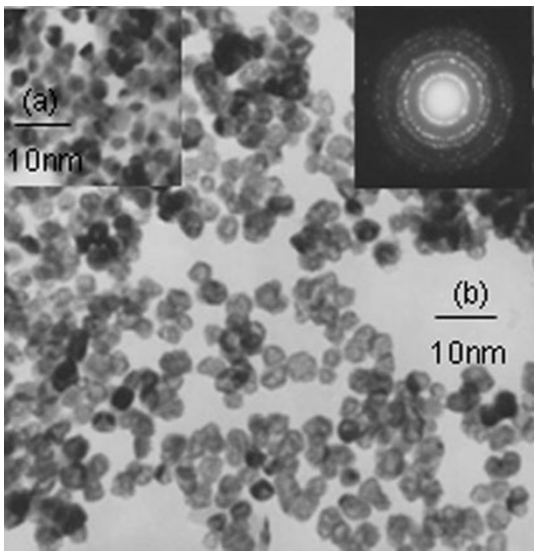

Fig. 6 TEM image of ZnS:Mn/$Zn(OH)_2$ nanocrystals (inset of left (A/W = 1:2) is bare ZnS:Mn and right is electron diffraction pattern of ZnS:Mn/$Zn(OH)_2$)

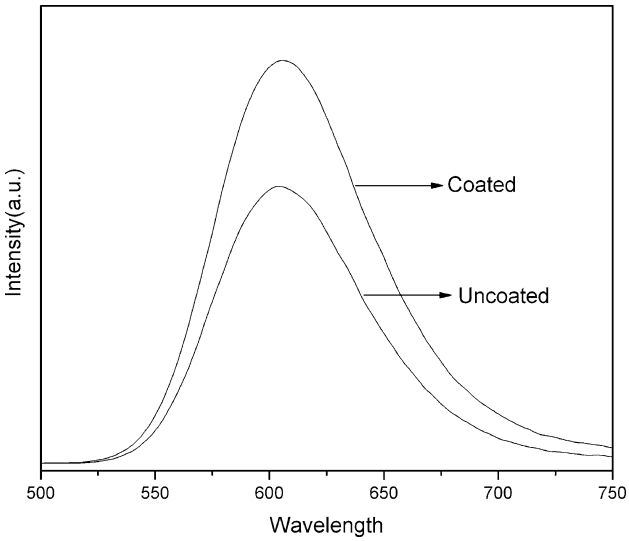

Fig. 7 The emission spectra of ZnS:Mn and ZnS:Mn/$Zn(OH)_2$ nanocrystals

calculated by following formula: $QY = {}^{Ec - Ea}/_{La - Lc}$, where Ec is the emission of sample, Ea is the emission of integrating sphere, La is the scatter of integrating sphere, and Lc is the scatter of sample, and after deducting the error of attenuating plate, the results are shown in Table 1. From Table 1, we find that the absolute quantum efficiency enhanced by 2.3% (from 8.4% of uncoated sample to 10.7% of coated sample). Based on the results, it is concluded that $Zn(OH)_2$ layer can passivate the surface of bare ZnS:Mn to improve the emission intensity and quantum efficiency.

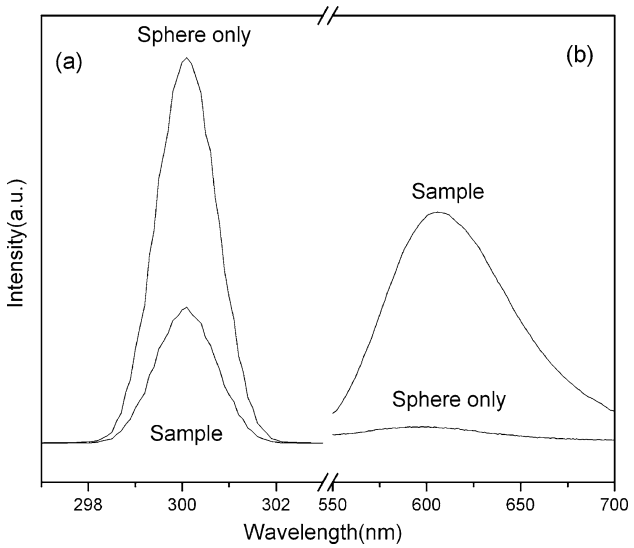

Fig. 8 The schematic representation of quantum efficiency measurement

Table 1 Quantum efficiency results

	Uncoated sample	Coated sample
Absorption	85.5%	88.0%
Absorbance	0.84	0.92
Quantum yield	8.4%	10.7%

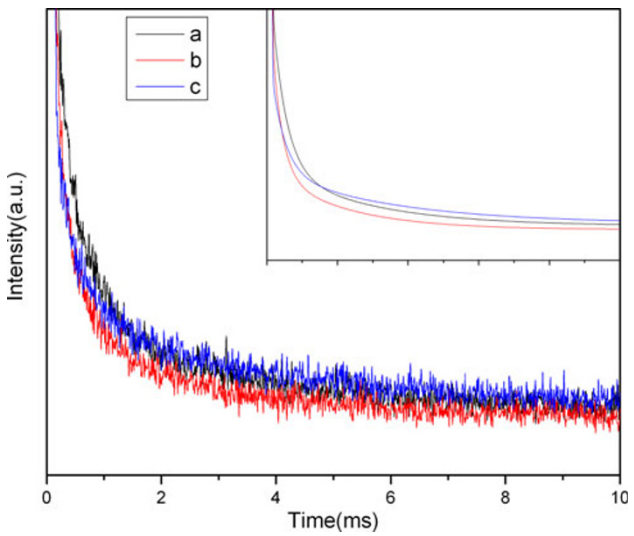

Fig. 9 The luminescent decay curves of samples

Luminescent decay curves and their fitting curves are shown in Fig. 9. Curves a, b, and c, respectively, represent the samples synthesized under conditions of A/W volume ratio of 1:1, 1:2, and coated with a layer of $Zn(OH)_2$ with

Table 2 Luminescent decay results

Samples	Lifetime
a	1.936
b	1.551
c	3.047

Mn-doped concentration of 2%. Because the Mn ions in ZnS host are insular luminescent centers, the decay is evidently required a multiexponential function, which is shown through the solid smooth line from the data.

$$y = B_1 \exp\left(-\frac{t}{\tau_1}\right) + B_2 \exp\left(-\frac{t}{\tau_2}\right) + B_3 \exp\left(-\frac{t}{\tau_3}\right) + y_0 \quad (8)$$

where, τ_1 is the lifetime of luminescence (at τ_1, the intensity decays to $e^{-1}$of its original intensity). Table 2 lists the lifetime of the luminescence at 605 nm of each sample. It can be found that shorter luminescent lifetime is fulfilled when A/W volume ratio is 1:2 with respect to 1:1. Sample coated with $Zn(OH)_2$ shell leads to the increased lifetime. As nonradiative recombination centers, recombination rate of the surface Mn ions is very fast. Once the number of the surface Mn ions is reduced by the $Zn(OH)_2$ shell, the nonradiative transition paths will be blocked to some extent, leading to the lengthen of the luminescence decay [28].

Conclusions

In summary, ZnS:Mn and ZnS:Mn/$Zn(OH)_2$ nanocrystals were synthesized by soft template and precipitation reaction method. As the Mn concentration increased, the emission intensity increases and reaches highest with the Mn content at 2%. Meanwhile, the emission intensity varies with the ratio of alcohol. When alcohol and water volume ratio is 1:2, the strongest emission intensity and shortest lifetime decay is achieved, which is attributed to the integrity of better particle getting from structure of alcohol/water template. When ZnS:Mn is coated with $Zn(OH)_2$, the emission intensity of Mn enhances by 30%, and its absolute quantum efficiency increases by 2.3%.

Acknowledgments This work was supported by the National Natural Science Foundation of China (10874061) and Research Fund for the Doctoral Program of Higher Education (200807300010).

References

1. L.E. Brus, J. Chem. Phys. **79**, 5566 (1983)
2. M. Bruchez Jr, M. Moronne, P. Gin, S. Weiss, A.P. Alivisatos, Science **281**, 2013 (1998)
3. V.L. Colvin, M.C. Schlamp, A.P. Allvisatos, Nature **370**, 354 (1994)
4. V.I. Klimov, A.A. Mikhailovsky, S. Xu, A. Malko, J.A. Hollingsworth, C.A. Leatherdale, H.J. Eisler, M.G. Bawendi, Science **290**, 314 (2000)
5. A.Y. Nazzal, L. Qu, X. Peng, M. Xiao, Nano Lett. **3**, 819 (2003)
6. S.C. Erwin, L. Zu, M.I. Haftel, A.L. Efros, T.A. Kennedy, D.J. Norris, Nature **436**, 91 (2005)
7. D.A. Schwartz, N.S. Norberg, Q.P. Nguyen, J.M. Parker, D.R. Gamelin, J. Am. Chem. Soc. **125**, 13205 (2003)
8. R.N. Bhargava, D. Gallagher, X. Hong, A. Nurmikko, Phys. Rev. Lett. **72**, 416 (1994)
9. D.J. Norris, N. Yao, F.T. Charnock, T.A. Kennedy, Nano Lett. **1**, 3 (2001)
10. Y. Hefetz, J. Nakahara, A.V. Nurmikko, L.A. Kolodziejski, R.L. Gunshor, S. Datta, Appl. Phys. Lett. **47**, 989 (1985)
11. A.A. Bol, A. Meijerink, J. Phys. Chem. B **105**, 10197 (2001)
12. M. Ohtaki, K. Oda, K. Eguchi, H. Arai, Chem. Commun. 1209 (1996)
13. V.V. Nikesh, S. Mahamuni, Semicond. Sci. Technol. **16**, 687 (2001)
14. W.X. Que, Y. Zhou, Y.L. Lam, Y.C. Chan, C.H. Kam, B. Liu, L.M. Gan, C.H. Chew, G.Q. Xu, S.J. Chua, S.J. Xu, F.V.C. Mendis, Appl. Phys. Lett. **73**, 2727 (1998)
15. M. Tan, W.P. Cai, L.D. Zhang, Appl. Phys. Lett. **71**, 3697 (1997)
16. H. Yanga, P.H. Holloway, B.B. Ratna, J. Appl. Phys. **93**, 586 (2003)
17. M. Tanaka, Y. Masumoto, Chem. Phys. Lett. **324**, 249 (2000)
18. S. Dixit, J. Crain, W.C.K. Poon, J.L. Finney, A.K. Soper, Nature **416**, 25 (2002)
19. H.-I. Chen, H.-Y. Chang, Colloids and surfaces a: physicochem. Eng. Aspects **242**, 61 (2004)
20. M. Tello, R. Garcia, Appl. Phys. Lett. **83**, 2339 (2003)
21. R.N. Bhargava, D. Gallagher, T. Welker, J. Lumin. **275**, 60 (1994)
22. K. Sooklal, B.S. Cullum, S.M. Angel, C.J. Murphy, J. Phys. Chem. **100**, 4551 (1996)
23. N. Pradhan, D. Goorskey, J. Thessing, X. Peng, J. Am. Chem. Soc. **127**, 17586 (2005)
24. R.J. Hunter, *Foundations of Colloid Science* (Clarendon Press, Oxford, UK, 1987), p. 443
25. Y. liu, X. Luo, Z. shen, J. li, X. ni, Opt. Rev. **13**, 303 (2006)
26. R. Chemama, J.J. Grob, A. Bouabellou, Mater. Sci. Eng. B **150**, 26 (2008)
27. L. Brus, J. Phys. Chem. **90**, 2555 (1986)
28. D. Jiang, L. Cao, G. Su, H. Qu, D. Sun, Appl. Surf. Sci. **253**, 9330 (2007)